Appendix 2 (article to be submitted to Habitation Journal or equivalent)

Flexible Microsensor Array for the Root Zone Monitoring of Porous Tube Plant Growth System

Sandeep Sathyan, D. Marshall Porterfield, H. Troy Nagle, Christopher S. Brown, Chang-Soo Kim*

Sandeep Sathyan, Chang-Soo Kim*: Departments of Electrical and Computer Engineering and Biological Sciences, University of Missouri-Rolla, Rolla, MO 65409, USA. 573-341-4529 (voice), 573-341-4532 (fax), ss6x7@umr.edu, ckim@umr.edu

D. Marshall Porterfield: Departments of Biological Sciences and Electrical and Computer Engineering, University of Missouri-Rolla, Rolla, MO 65409, USA. 573-341-6336 (voice), 573-341-4821 (fax), mporterf@umr.edu

H. Troy Nagle: Biomedical MicroSensors Laboratory, Department of Electrical and Computer Engineering, North Carolina State University, Raleigh, NC 27695-7911, USA, 919-515-3578 (voice), 919-513-3814 (fax), t.nagle@ncsu.edu

Christopher S. Brown: Kenan Institute for Eng., Tech., & Science, North Carolina State Univ., USA. 919-515-5118 (voice), 919-515-5831 (fax), cbrown@ncsu.edu

* Corresponding author

ABSTRACT

Control of oxygen and water in the root zone is vital to support plant growth in the microgravity environment. The ability to control these sometimes opposing parameters in the root zone is dependent upon the availability of sensors to detect these elements and provide feedback for control systems. In the present study we demonstrate the feasibility of using microsensor arrays on a flexible substrate for dissolved oxygen detection, and a 4-point impedance microprobe for surface wetness detection on the surface of a porous tube (PT) nutrient delivery system. The oxygen microsensor reported surface oxygen concentrations that correlated with the oxygen concentrations of the solution inside the PT when operated at positive pressures. At negative pressures the microsensor shows convergence to zero saturation (2.2 μmol/L) values due to inadequate water film formation on porous tube surface. The 4-point microprobe is useful as a wetness detector as it provides a clear differentiation between dry and wet surfaces. The unique features of the dissolved oxygen microsensor array and 4-point microprobe include small and simple design, flexibility and multipoint sensing. The demonstrated technology is anticipated to provide low cost, and highly reliable sensor feedback monitoring plant growth nutrient delivery systems in both terrestrial and microgravity environments.

Keywords – Dissolved oxygen microsensor, porous tube, plant nutrient solution delivery, conductivity, polyimide.

I. INTRODUCTION

In space farming, plants can effectively provide food and recycle air, wastes and water to support long-term manned exploration [1]. Currently the most challenging aspects of supporting plant growth in microgravity environments are controlling water, mineral nutrients, and oxygen bioavailability in the root zone and rhizosphere. An important aspect of this system to consider is we do know that water content and oxygen are inversely opposed due to chemical and physical limitations associated with oxygen in the liquid phase. Also the performance of the nutrient delivery system in microgravity may be altered as forces such as surface tension, atmospheric pressure and capillary action would come to dominate the system in the partial or complete absence of gravity [1, 2]. As a result of this space based experiments have demonstrated that microgravity conditions cause biophysical limitations leading to hypoxia in plant roots [3, 4]. Additionally, buoyancy driven convection is inhibited in microgravity, and this would functionally limit oxygen and dissolved solute transport to the relatively slow process of diffusional flux to provide gas exchange for metabolism. Due to these problems passive, open loop control of plant nutrient delivery subsystems are not adequate and instead active systems for the delivery of oxygen, water and nutrients are required. Closed loop controls, driven by sensor inputs will also be required as water and gas content of the rootzone are inversely related and require careful balance in order to insure optimized performance.

One of the critical operational requirements of a plant nutrient delivery system in microgravity is to provide effective fluid delivery system while preventing free liquid release into the cabin where it might be lost or damage other equipment [5]. As a result of this requirement plant nutrient delivery modules are effectively sealed. While this does not impede the systems effective ability to provide a uniform distribution of water and nutrients within the root zone it is another limiting design factor that might impact our ability to maintain adequate oxygen levels. Some engineers and biologists have considered this and designed passive nutrient delivery systems that allow for maintenance of water under controlled conditions, but these passive systems do not necessarily address biophysical problems with delivery of metabolic gasses to the root tissue [6]. Advanced active hydroponic systems have been proposed and developed, and one system that is being tested is the hydroponic porous tube plant nutrient delivery system as shown in figure 1 [7, 8, 9]. This porous tube provides efficient capillary interface between plant nutrient

solution and plant roots allowing provision of adequate levels of water and nutrients to the root zone [10, 11]. Precise monitoring and control of these parameters are required to avoid oxygen deficiency or insufficient aeration in the root zone area. To achieve this, advanced sensors having features such as small size, reliability, robustness, flexibility, easy calibration and biocompatibility have to be developed to provide exceptional benefits when used in plant growth system.

Other works by engineers and scientists have been directed at the development of advanced sensors for use in control of plant nutrient delivery systems. For example the Water Availability Sensor (WAS) was designed to measure water thickness on a PT surface based on infrared principles [2]. Other water sensors have been used based on resistance measurements [5] and also changes in thermal capacitance and thermal conductance [12]. These sensors were designed to meet some of the requirements of ideal sensors but only did so with limited success. Recent trends in sensor technology are based on the development of multifunctional and multipoint sensors that can be incorporated as on-chip intelligent and integrated sensors. Due to bulky and rigid designs the earlier sensors are incompatible and cannot be used as smart sensors incorporated on-chip, for small localized measurements.

Very few studies involving plant growth have shown the utilization of dissolved oxygen sensors for determining root zone activity. Commercially available Clark type and Whalen type electrodes are designed to be stir insensitive and sensitive only to diffusion based oxygen transport [13]. They have a hydrophobic membrane applied over the cathode. This ensures that the oxygen consumption in the electrode does not effect the oxygen concentration in the medium being measured. What this means is in microgravity, standard oxygen concentration sensors cannot be used as it cannot detect oxygen changes in non-diffusion based transport. The only way they can appropriately be used is where exact placement of the sensor and standardization of the system would be possible, in order to insure proper control feedback. Given the fact that amperometric oxygen sensors are fragile and/or bulky there use in these situations would be limited. A novel approach to this problem is the development of a biomimetic Root Oxygen Bioavailability (ROB) sensor, which has been used to directly measure changes in oxygen bioavailability in microgravity, when oxygen concentrations were constant [4]. For the present work our sensor was developed based on a flexible amperometric microsensor array. The sensor functions through the electrochemical reduction of oxygen and is flexible, miniature and robust in order to be used for direct measurement of oxygen concentrations on the surface of a PT. This array also includes a 4-point conductivity microprobe for wetness detection on the surface of porous tube plant nutrient delivery system. With its unique features (small and simple

structure, flexibility and multipoint sensing), the 4-point microprobe and dissolved oxygen microsensor array can be used to measure oxygen concentrations under standardized conditions that would not be possible with other electrochemical oxygen sensors.

II. METHODS

1. Microsensor preparation

We designed an amperometric dissolved oxygen sensor based on the 3-electrode electrochemical cell configuration and a conductivity probe based on the 4-point impedance cell configuration. The 3-electrode cell minimizes the ohmic voltage drop through the electrolyte between the anode and cathode and prevents the consumption of reference electrode material (usually Ag/AgCl) [14]. Our electrochemical cell design, as in figure 2(a), comprises of concentric electrodes to ensure symmetric diffusional mass transport of electrochemical species in all radial directions. The center electrode serves as the reference electrode (RE) with an exposed diameter of 100 μm . Proceeding from inside to outside, the next concentric circle is used as the working electrode (WE). This is the site at which dissolved oxygen molecules are cathodically reduced. The outermost circle is the counter electrode (CE). The working electrode and counter electrode have a width of 50 μm each with their exposed surface areas being 3.8E-04 cm^2 and 7.6E-04 cm^2, respectively. The spacing between two successive concentric electrodes is 100 μm. The overall microsensor has a diameter 0.9 mm. The dissolved oxygen sensor strip made of flexible polyimide substrate consists of 4 microsensors as in figure 2(b). The strip is 58 mm long and 6 mm wide. This length enables the placement of sensors at equidistance of 10 mm when they are enwrapped on the porous tube surface. The 4-point conductivity sensor strip consists of 4 identical electrodes of diameter 500 μm with the outer pair of electrodes acting as current probes and the inner pair acting as voltage probes, respectively. The spacings between the current probes and the voltage probes are 80 mm and 76 mm, respectively.

All of the prototype sensors were fabricated in the facilities of the Biomedical Microsensors Laboratory (BMMSL) at North Carolina State University [15]. All the electrodes are made of platinum. On the Kapton® (polyimide) substrate, a thin film of chromium as an adhesion layer was first deposited. Platinum was deposited subsequently on the chromium layer. The metal layers were defined by conventional photolithography process. Then photosensitive polyimide was spin-coated and developed to encapsulate the platinum electrodes. Electroplating of Ag/AgCl on the reference electrode was carried out in a two step process. The first step involves silver plating on

platinum electrode with 1 wt% $KAg(CN)_2$ (1 g in 99 ml H_2O) as the plating solution. A constant current source (Keithley 225) was used to generate a constant current density of 0.25 mA/cm^2 for 10 minutes. The plating solution was magnetically stirred for uniform silver electroplating. In the second step, chloridation is achieved over the electroplated silver layer using 0.1 M NaCl as electrolyte with a current density of 0.25 mA/cm^2 for 3 minutes. For both the steps, platinum wire was used as counter electrode. The fabricated sensor was coated with poly-HEMA (poly 2-hydroxyethyl methacrylate), a hydrophilic membrane, by dipping method. This layer reduces stir sensitivity and acts as a protective membrane.

2. Setup

The plant nutrient delivery system shown in figure 3 includes a 1 liter liquid reservoir to store the plant nutrient solution. A gear pump (Cole Parmer, 7521-50) is utilized to draw out the solution from the reservoir and into the alumina porous tube (Refractron, porosity 0.5 μm, outer diameter 13 mm, inner diameter 8 mm, length 100 mm) at a constant flow rate of 15 ml/min. The internal pressure of the tube can be either positive or negative depending on the polarity of the pump direction. A valve on each side of the tube controlled the internal pressure between -4 kPa to +4 kPa. Two pressure gauges (3D instruments, DTG-6000) at each of the inlet and outlet terminals of the porous tube provided the internal pressure reading. The pressure difference between the input and the output of the tube was negligible. Dissolved oxygen level on the porous tube surface was monitored using a commercial Clark type oxygen probe (Harvard/Instech, AH-56-5002, diameter 3.2 mm, length 41.3 mm). The permeable hydrophobic membrane and internal electrolyte of the commercial probe were replaced once for every experimentation cycle. The oxygen microsensor array was connected to the instrument using a zero-insertion force connector as shown in the picture in figure 3. Initially the microsensor was placed in a measuring vessel and pre-polarization of the sensor was performed for 15-20 minutes before the actual measurements. Later, the microsensor array was applied on the porous tube and the calibration and measurements were performed at different oxygen saturation\concentration levels of internal solution and different internal pressures. The flexible oxygen microsensor array is enwrapped around the porous tube as in figure 4(a) whereas the 4-point electrodes are placed on the surface along the length of the tube as in figure 4(b). The outer pair of current probes minimizes the influence of contact impedance of the voltage probes during the impedance measurement. All measurements were performed at room temperature (23° C ± 1° C).

3. Instrumentation

A custom set of electrochemical instrumentation has been employed for experiments involving the microsensor. A potentiostat (Gamry Instruments, PC4-FAS1) was used along with a multiplexer (Gamry Instruments, ECM8) to individually address the 4 oxygen microsensors in a strip. A separate source-measure unit (Keithley Instruments, SCS-4200) was used to measure oxygen responses with the commercial probe. To equilibrate the solution to the desired oxygen saturation level, a fixed ratio of oxygen and nitrogen gases were bubbled in the reservoir using two mass flow controllers (MFC) (MKS Instruments, 1159B). The operation of the MFC was controlled using a 4 channel readout power supply (MKS Instruments, 247C). A potentiostat (Gamry Instruments, PC4-750) was used to perform the 4-point impedance measurements. Electrochemical characterization of the microsensor was performed using linear sweep voltammetry (LSV) and chronoamperometric (CA) methods. The LSV was used to determine the cathode oxygen reduction voltage of the working electrode. The CA measurements were made to obtain the oxygen responses with respect to time. The conductivity measurement was performed with a current density of 0.1 mA/cm^2 (rms) at the frequency of 1 kHz.

III. RESULTS AND DISCUSSION

1. Electrochemical characterization in bulk solution

Microsensor characterization was performed in plant nutrient solution (quarter strength Hoagland's solution, pH 5.8–6). LSV measurements were made over a voltage range of 0.0 to -1.0 V at a step decrement of 50 mV/s starting at 0 V. For potentials between 0 to -0.6 V, reaction rates were dependent on both rates of charge transfer of oxygen reduction as well as mass transport of oxygen towards cathode. For potentials between -0.6 to -0.8 V, the limiting current plateau was observed which implies that the reaction rate was determined by only the mass transport. For any lower potential, hydrogen evolution due to water decomposition causes a steep increase in current. So the cathodic potential for oxygen reduction was chosen as -0.7 V vs. Ag/AgCl as it has a minimum reduction of species other than oxygen [16]. Chronoamperometric measurements were performed and the resultant transient responses of the microsensor, for varying oxygen saturation levels (concentrations), are shown in figure 5(a). The response time to achieve steady-state limiting current was about 20 seconds. The corresponding calibration curve is shown in figure 5(b). The sensor response is plotted both in terms of oxygen concentration (μmol/L) as well

as gas phase oxygen saturated in nutrient solution (%). During conversion of values from gas phase oxygen saturated in solution to oxygen concentration, a salinity factor of 2.3 g/L for the Hoagland's solution is taken into consideration. The sensor response is linear and repeatable over the gas phase oxygen saturation range of 0 % (2.2 μmol/L) to 50 % (521.9 μmol/L). This is in agreement with the limiting current theory where the relationship between limiting current magnitude and oxygen concentration is linear [14, 16]. But the linearity is not maintained well over the gas phase 50 % oxygen saturation level (i.e. 521.9 μmol/L O_2 concentration). This could be attributed to a possible reduction of oxygen catalytic activity due to increase in the local pH near the working electrode at higher oxygen level [16]. The limiting current in unstirred bulk plant nutrient solution was approximately 50 % lower than stirred solutions as in figure 5(a). The slope of the calibration curve is higher for stirred condition, as in figure 5 (b), showing that the nutrient solution is well replenished and having higher mass transport rate when compared to unstirred condition. Importantly, it is noted that when the sensor is in direct contact with the porous tube the stir sensitivity would be reduced to a great extent or eliminated. Bare sensors exhibited higher currents than sensors with poly-HEMA coating as the mass transport rate was higher without this hydrophilic coating. A small amount of residual current was observed at zero saturation (2.2 μmol/L O_2 concentration) level.

2. Oxygen microsensors:

A commercial Clark type dissolved oxygen probe was initially used to serve as a reference for the microsensor results. A 2-point calibration was performed on the porous tube surface at 2.2 μmol/L and 178.1 μmol/L oxygen concentrations that correspond to 0% and 20 % O_2 gas bubbled in internal solution at the highest positive pressure (3.0 kPa). All data points in figure 6(a) were based on these calibration points, since the reliable calibration procedure was possible only when the probe was bathed in a sufficient water film in positive pressure. Therefore probe responses at higher positive internal pressures properly reflect the oxygen concentration value of the inner solution. At lower positive pressures less water film will be formed and subsequently the probe will be only partially in contact with the internal solution and partially exposed to the gaseous oxygen in air (21 %). Thus the responses start to show reduced sensitivity to dissolved oxygen in the water film. At zero pressure and negative internal pressures, the probe response converges to air saturation values. This is because there will be little water film on the tube surface and the sensor response is mainly affected by the gaseous oxygen available from the environment owing to negligible stirring sensitivity of the commercial probe. But the extremely little presence of

water film at zero or negative pressures leads to a deviation of the probe response away from the air saturation value. Figure 6(b) shows the linear calibration response of the probe depending on the internal pressure. When little water film is formed on the tube surface (i.e. negative or zero pressure), the calibration curve exhibits almost zero slope. As the film thickness is increased, the slope of the calibration curve gradually increases as the internal solution comes into contact with the probe surface. The maximum slope is observed when enough water film is formed on the tube at high positive pressures.

The microsensor characterization was performed in a similar manner as the commercial probe. It was first subjected to prepolarization (preconditioning) for 15-20 minutes before the actual measurement and then subjected to chronoamperometric tests. Each sensor in a strip was separately multiplexed by the pulsatile cathodic oxygen reduction voltage. The calibration was performed by bubbling gaseous oxygen at 0 % and 20 % O_2 in nutrient solution (i.e. 2.2 μmol/L and 178.1 μmol/L oxygen concentrations respectively) on the tube surface at the highest pressure (3.0 kPa). The microsensor response, shown in figure 7(a), was similar to the commercial probe response at positive pressure. The response curve value, for a fixed oxygen saturation level, increases as water film thickness on the surface increases. The microsensor reflects oxygen levels properly with enough water film on the tube surface. It should be noted that, however, the sensitivity almost saturated in a less positive pressure (1.5 kPa). This fact implies that the thin film microsensor is useful for oxygen detection with very small sample amount or in microscale local environment. But the responses at negative pressures were scattered around the 2.2 μmol/L oxygen concentration value and measurements were not reliable due to surface dryness and absence of sensor hydrophobic membrane of the Clark type sensor. There can be another reason for the decreasing sensitivity at lower pressures. As shown in figure 5(b), the microsensors showed higher sensitivity towards stirring than commercial probes due to the absence of a hydrophobic membrane. Since the calibration was performed once at highest positive pressure only, the probe response deviates from the actual values as the pressure decreases due to varying stirring conditions. Therefore, the deviation along with scattering is significant at zero and negative pressures due to both stirring effect and insufficient water film. But at positive pressures, problems arising due to insufficient water film are not much significant compared to stirring effect. The calibration curve in figure 7(b) shows that the slope is positive whenever there is a presence of water film on the porous tube surface and increases with increase in the liquid film thickness for a fixed oxygen concentration level. Further increase of the film thickness, by increasing the internal pressure of the porous tube, will not yield any substantial increase in the slope of the calibration curve.

3. Conductivity microprobe:

When the surface is dry, impedance between the probes is very high as there is no suitable conducting medium (plant nutrient solution). Gradual decrease of impedance in negative pressure region as shown in figure 8 implies that the water content within the porous tube media is increasing due to the decreasing suction capability. This result suggests a possibility of using the conductivity probe in measuring the moisture contents in unsaturated particulate plant growth media in combination with pulse moisture sensor [12]. A steep transition towards lower impedance value at the moderate negative pressure is considered to be due to the capillary effect to contain the solution in the porous tube media. Once the pore portion in the tube is saturated with solution solely by the capillary force in the zero pressure, the impedance showed almost the least value. This implies that the contribution of surface water film to conductivity is negligible compared to that of saturated porus media. For positive pressures, there is no clear differentiation between the different levels of liquid film thickness on the wet tube surface. The results for both 2-probe and 4-probe impedance measurements were compared and it was found that 4-probe demonstrates lower average impedance values along with higher percentage of difference between wet and dry surface values by minimizing the effect of contact impedance between the electrode and the solution.

IV. CONCLUSION

First, a microfabricated dissolved oxygen sensor array is presented. For space missions, it is desirable to have dissolved oxygen sensors that can measure oxygen concentrations in a way that is standardized and prevents artifacts associated with the spaceflight environment. While this sensor does not directly measure oxygen bioavailability in root zone, it does directly measure oxygen concentrations in the root zone, without having water content or root growth in the immediate sensor zone to impact these measurements. The response of the oxygen microsensor is comparable with the performance of the commercial Clark type probe on the tube surface with regard to oxygen concentration measurements. The microsensors work effectively in the presence of water film. The results suggest that the microsensors are capable of determining oxygen saturation on the porous tube surface, where the stir-sensitivity of sensor would be minimized, yet would insure maximum sensitivity. Additionally, a 4-point microprobe for wetness detection in the porous tube system is discussed. The 4-point impedance probes clearly differentiate between wet and dry surfaces. Results suggest that the microprobes are capable of determining porous

media wetness on the porous tube surface. These microsensors and microprobes could be employed for plant root zone monitoring in varied fluid delivery systems that are being developed especially the porous tube nutrient delivery system and the particulate based system. Further sensor developments are focused on achieving enhancement of integrated microsensors along with on-chip structural integration in monitoring systems.

ACKNOWLEDGEMENTS

This research was supported by a grant from the NASA Office of Biological and Physical Research (01-OBPR-01).

REFERENCES

1. Monje,O.; Stutte,G.W.; Goins, G.D.; Porterfield, D.M.; Bingham, G.E., Farming in Space: Environmental and Biophysical Concerns. Advanced Space Research Vol. 31: 151-167; 2003.
2. Dreschel, T.W.; Carlson, C.W.; Wells, H.W.; Anderson, K.F., Physical testing for the microgravity plant nutrient experiment. Paper No 93-4007, American Society of Agriculture Engineers, Spokane, Washington; 1993.
3. Porterfield, D. Marshall, The biophysical limitations in physiological transport and exchange in plants grown in microgravity. Journal of Plant Growth Regulation. 21: 177-190; 2002.
4. Liao, J., Liu, G., Monje, O., Stutte, G.W., Porterfield, D.M., Induction of hypoxic root metabolism results from physical limitations in O2 bio-availability in microgravity. Adv. Space Res. , 2004.(In press)
5. Levine, Howard; Piastuch, W.C; Dreschel, T.W., Development of a microgravity rated hydroponic plant culture apparatus. Proceedings of the 36th Space Congress: 295-302; 1999.
6. Porterfield, D.M.; Dreschel, T.W.; Musgrave, Mary E., A ground based comparison of nutrient delivery technologies developed for growing plants is spaceflight environment. HortTechnology 10: 179-185; 2000.
7. Dreschel, T.W.; Brown, C.S.; Piastuch, W.C.; Knott, W.M., Porous tube plant nutrient delivery system development: A device for nutrient delivery in microgravity. Advanced Space Research Vol. 14: (11)47-(11)51; 1994.

8. Burtness, Kevin; Norwod, Kelly; Murdoch, Trevor; Levine, Howard, Development of a porous tube based plant growth apparatus. Paper No. 2002-01-2389, 32nd International Conference on Environmental Systems, San Antonio TX; 2002.
9. Dreschel, T.W.; Brown, C.S.; Piastuch, W.C.; Hinkle, C.R., A summary of porous tube plant nutrient delivery system investigations from 1985 to 1991. NASA Technical Memorandum 107546, Jan 1992.
10. Tsao, David T.; Okos, Martin R.; Sager, John C., Controlling the water availability from a ceramic tube system subjected to non-standard gravities. SAE Technical paper series #961505, Monterey CA; 1996.
11. Dreschel, T.W.; Sager, John C., Control of water and nutrients using a porous tube: A method for growing plants in space. HortScience, Vol. 24: 944-947; 1989.
12. Clark, G.J.; Neville, Jr.; Dreschel, T.W., A root moisture sensor for plants in microgravity. Advanced Space Research, Vol. 14: (11)213-(11)216; 1994.
13. Schneiderman, Gary; Goldstick, Thomas K., Oxygen electrode design criteria and performance characteristics: recessed cathode. Journal of applied physiology, Vol. 45: (1)145-(1)154; 1978.
14. Lambrechts, M.; Sansen, W., Biosensors: microelectrochemical devices, IOP Publishing, 1992.
15. Buck, R.P.; Lindner, V.V.Cosofret; Ufer, S.; Madaras, M.B.; Johnson, T.A.; Ash, R.B.; Neuman, M.R., Microfabrication technology of flexible membrane-based sensors for in-vivo applications. Electroanalysis, Vol. 7: 846-851; 1995.
16. Linek, V.; Vacek, V.; Sinkule, J.; Benes, P., Measurement of Oxygen by Membrane-covered Probes. Ellis Horwood; 1988.

FIGURE CAPTIONS

Figure 1. Porous tube nutrient delivery system in microgravity. The plants are grown on the porous tube surface and the nutrient solution is delivered to the root zone through the pores in the tube by capillary force. The system efficiently ensures no free liquid escapes, provides a uniform distribution of water and nutrients within the root zone and maintains adequate oxygen levels at root zone. The porous tube provides efficient capillary interface between plant nutrient solution and plant roots.

Figure 2. (a) Cross-section of 3-electrode amperometric oxygen microsensor on flexible polyimide (Kapton®) substrate (1. substrate cleaning, 2. metallization of Pt/Cr and photolithography, 3. polyimide photolithography). The 3-electrode cell minimizes the ohmic voltage drop through the electrolyte between the anode and cathode and prevents the consumption of reference electrode material. Cell design comprises of platinum concentric electrodes to ensure symmetric diffusional mass transport of electrochemical species in all radial directions. The center electrode serves as the reference electrode (RE) (exposed diameter of 100 μm). This is later electroplated with Ag/AgCl on the reference electrode The next concentric circle is used as the working electrode (WE). The spacing between two successive concentric electrodes is 100 μm., **(b)** Photograph of the oxygen microsensor strip including an array of 4 sensors. The dissolved oxygen sensor strip made of flexible polyimide substrate consists of 4 microsensors. The strip is 58 mm long and 6 mm wide. This length enables the placement of sensors at equidistance of 10 mm when they are enwrapped on the porous tube surface.

Figure 3. A schematic of the plant nutrient delivery system and the associated instrumentation. The system includes a 1 liter liquid reservoir to store the plant nutrient solution. A gear pump draws out the solution from the reservoir and into the alumina porous tube (Refractron, porosity 0.5 μm, OD 13 mm, ID 8 mm, length 100 mm) at a constant flow rate of 15 ml/min. The internal pressure of the tube can be either positive or negative depending on the polarity of the pump direction. A valve on each side of the tube controls the internal pressure between -4 kPa to +4 kPa. Two pressure gauges (3D instruments, DTG-6000) at each of the inlet and outlet terminals of the porous tube provide the internal pressure reading. A closer look at the oxygen microsensor strip enwrapped around the porous tube and attached to the connector.

Figure 4. (a) Cross-section of the porous tube with the oxygen microsensor strip (with 4 microsensors) enwrapping with the sensor in contact with the tube surface. The 4 sensors are placed equidistant from each other on the surface., **(b)** 4-probe conductivity microprobe placed along the surface with probes 1 and 4 as current probes and probes 2 and 3 as voltage probes, respectively. Each identical electrode has a diameter 500 μm. The spacing between the current probes and the voltage probes are 80 mm and 76 mm, respectively. The outer pair of current probes minimizes the influence of contact impedance of the voltage probes during the impedance measurement. All measurements were performed at room temperature (23° C ± 1° C).

Figure 5. (a) Typical transient chronoamperometry responses of oxygen microsensor for an applied cathodic potential of -0.7 V vs. Ag/AgCl at different oxygen concentration levels (with their corresponding gas phase oxygen saturation values) in plant nutrient solution (quarter strength Hoagland's solution, pH 6.0, room temperature) for stirred and unstirred conditions. The sensor response is linear and repeatable over the gas phase oxygen saturation range of 0 % to 50 % O_2 (i.e. 2.2 μmol/L to 521.9 μmol/L O_2 concentration). **(b)** Calibration curve from the limiting current values measured at time = 30 seconds in the chronoamperometry test. The limiting current in unstirred bulk plant nutrient solution shows approximately 40 % lower values than stirred solutions showcasing the microsensor's stir sensitivity. The slope of the calibration curve is higher for stirred condition when compared to unstirred condition.

Figure 6. (a) Surface dissolved oxygen measurement with a commercial Clark-type mini-probe with respect to different internal pressures of nutrient solution within the porous tube with different oxygen concentration levels (with the corresponding gas phase oxygen saturation in solution values) of inner nutrient solution. Probe responses at higher positive internal pressures properly reflect the oxygen value of the inner solution. Thicker water films are not easily affected by gaseous oxygen in air (21%). As water film thickness decreases, probe responses start converging to air saturation values., **(b)** Replot of (a) with respect to different oxygen concentration levels to show the sensitivity depending on the internal pressure. With little water film formed on the tube surface (i.e. negative or zero pressure), the calibration curve exhibits almost zero slope. As the film thickness increases, the slope of the calibration curve gradually increases as the internal solution comes into contact with the probe surface.

Figure 7. (a) Surface dissolved oxygen measurement with a microsensor array with respect to different internal pressures of nutrient solution within the porous tube with different oxygen concentration levels of inner nutrient. The response curve value, for a fixed oxygen concentration level, increases as water film thickness on the surface increases. The microsensor reflects oxygen levels properly with enough water film on the tube surface. The responses at negative pressures are scattered around the lowest oxygen concentration value and measurements are not reliable due to surface dryness and absence of sensor hydrophobic membrane., **(b)** Replot of (a) with respect to oxygen saturation\concentration levels to show the sensitivity depending on the internal pressure. The calibration

curve shows that the slope is positive whenever there is a presence of water film on the porous tube surface and increases with increase in the liquid film thickness for a fixed oxygen concentration.

Figure 8. Surface wetness measurement with a 4-point microprobe showing a gradual decrease of surface impedance at the transition from negative to positive pressure. Dry surface shows higher impedance between the probes as there is no suitable conducting medium. Gradual decrease of impedance in negative pressure region implies that the water content within the porous tube media is increasing due to the decreasing suction capability. Steep transition towards lower impedance value at the moderate negative pressure is due to the capillary effect to contain the solution in the porous tube media. Impedance is least when the pore portion in the tube is saturated with solution.

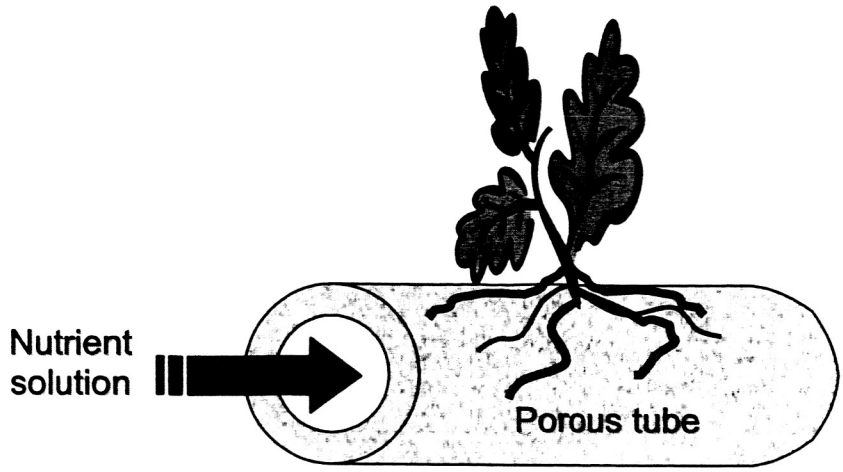

Figure 1

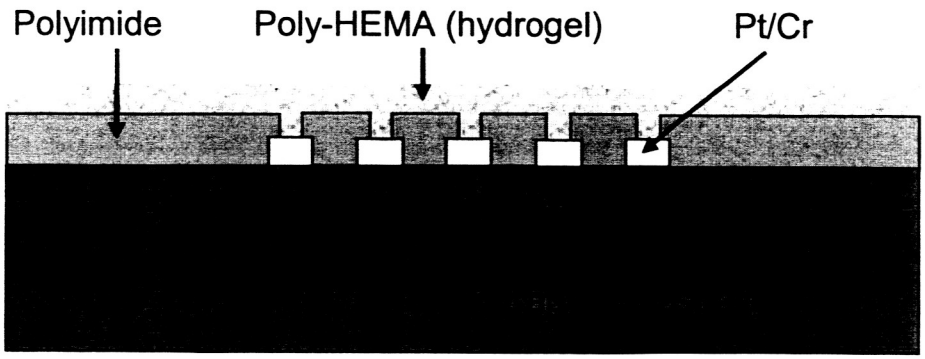

(a)

(b)

Figure 2

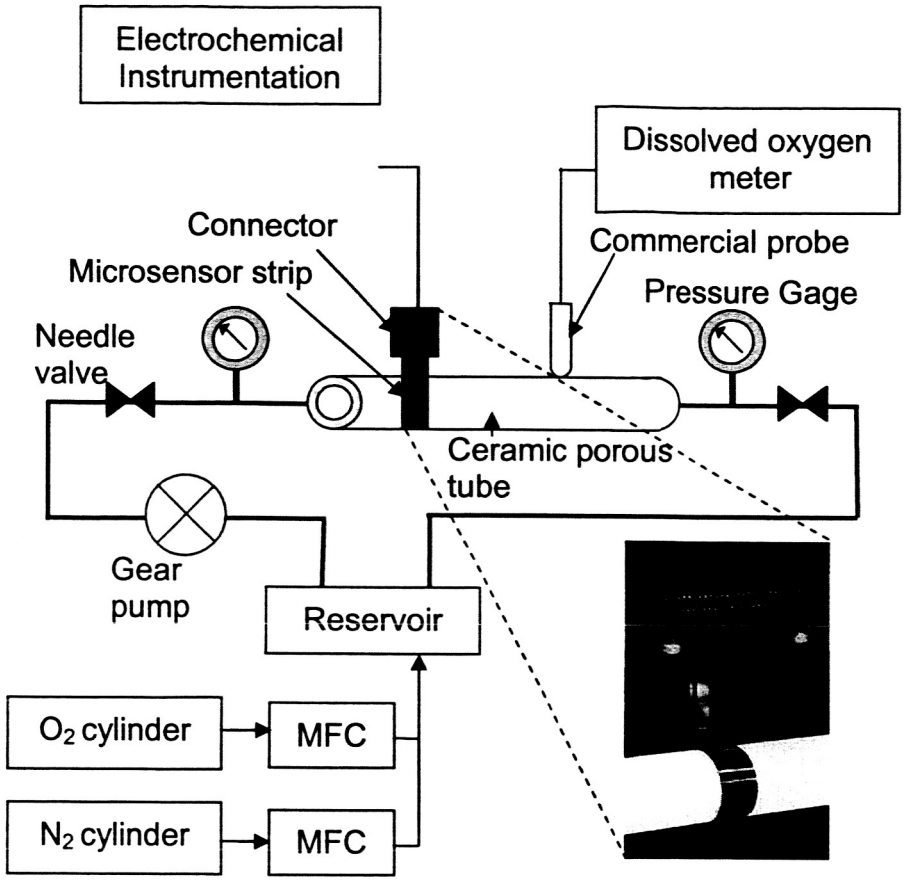
Electrochemical Instrumentation
Dissolved oxygen meter
Connector
Microsensor strip
Commercial probe
Pressure Gage
Needle valve
Ceramic porous tube
Gear pump
Reservoir
O_2 cylinder
MFC
N_2 cylinder
MFC

Figure 3

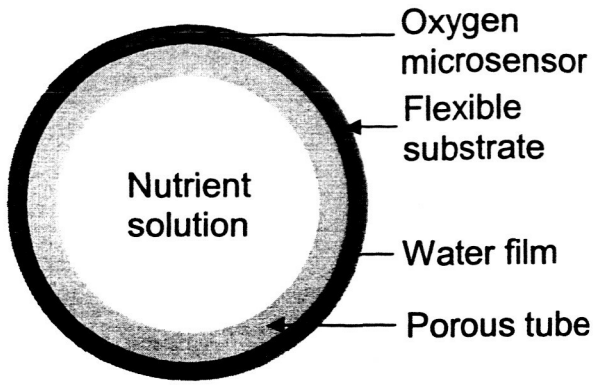

Transversal cross-section

(a)

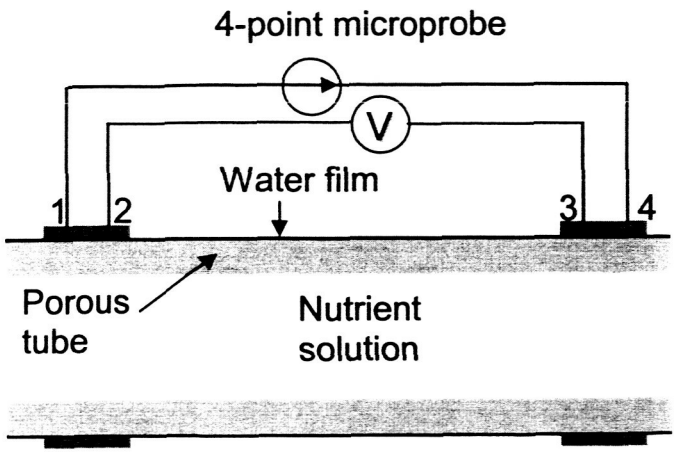

Longitudinal cross section

(b)

Figure 4

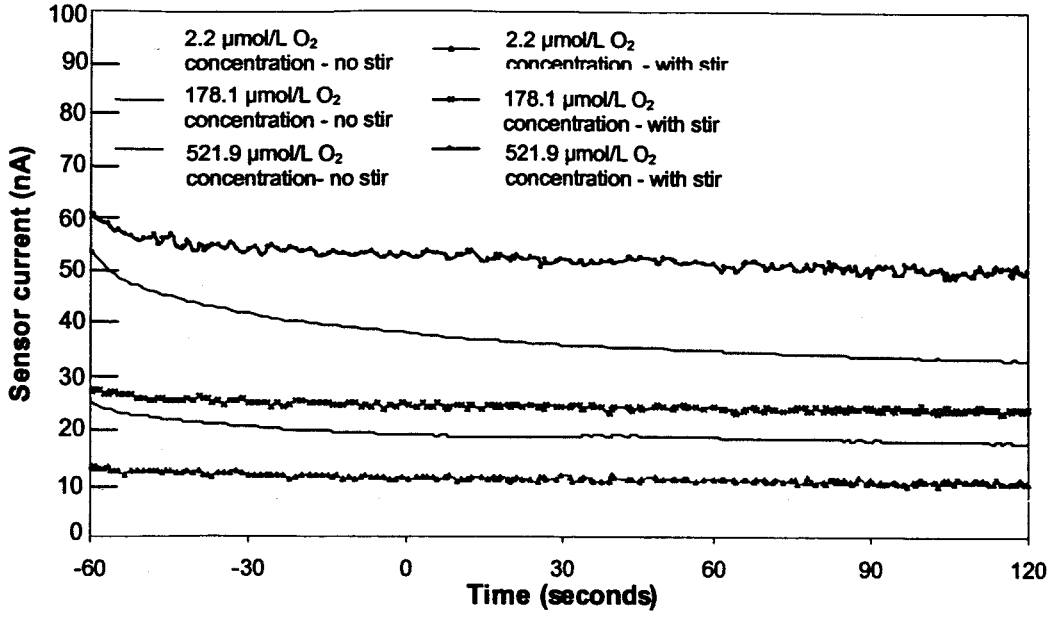

(a)

Figure 5 (a)

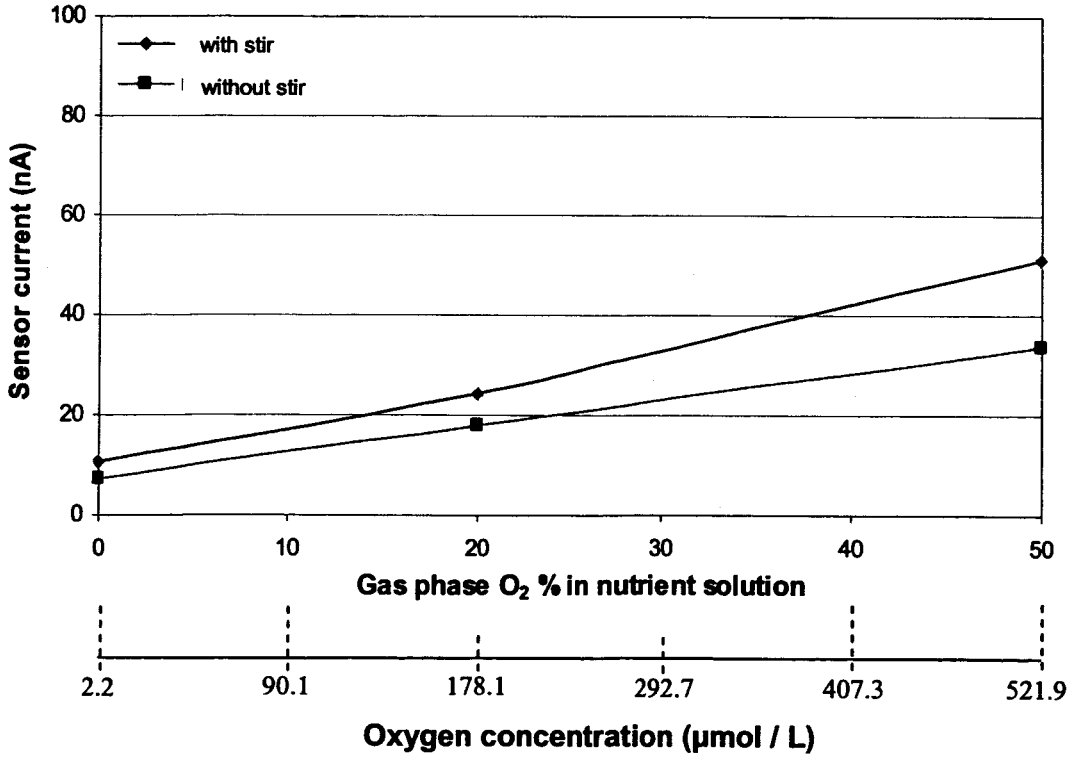

(b)

Figure 5 (b)

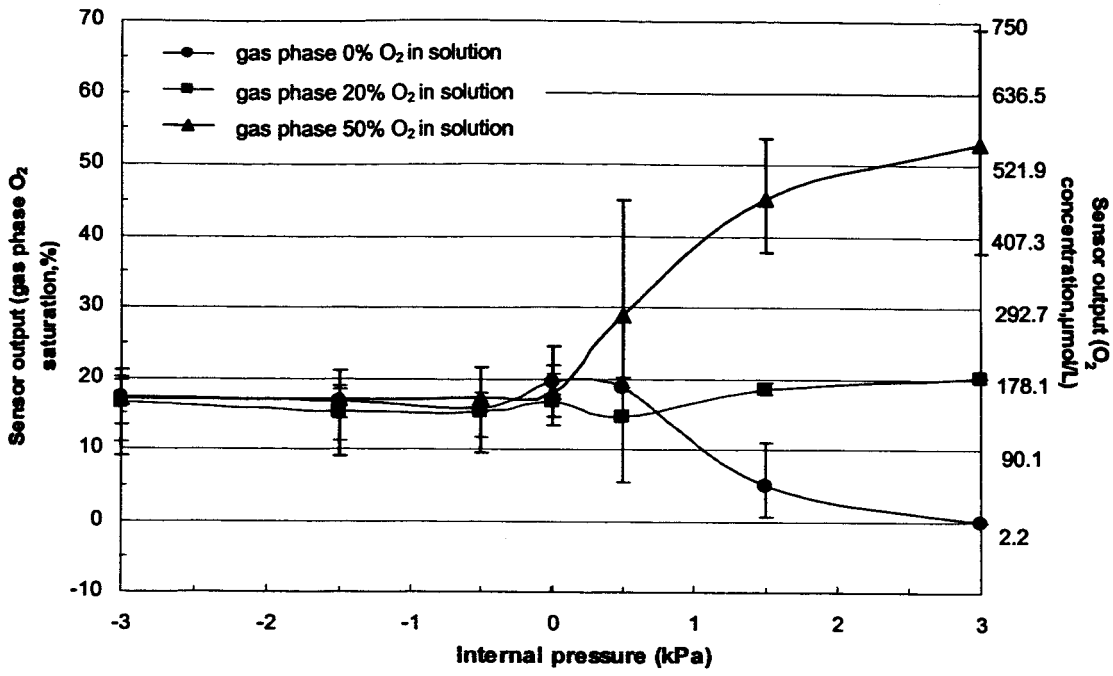

(a)

Figure 6 (a)

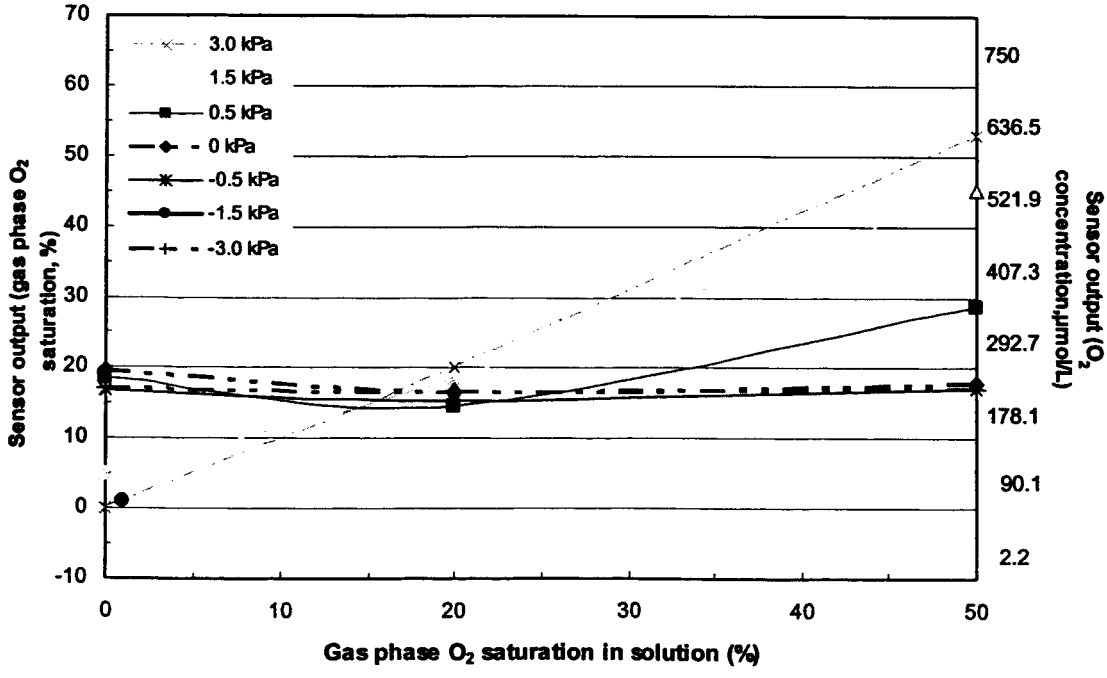

(b)

Figure 6 (b)

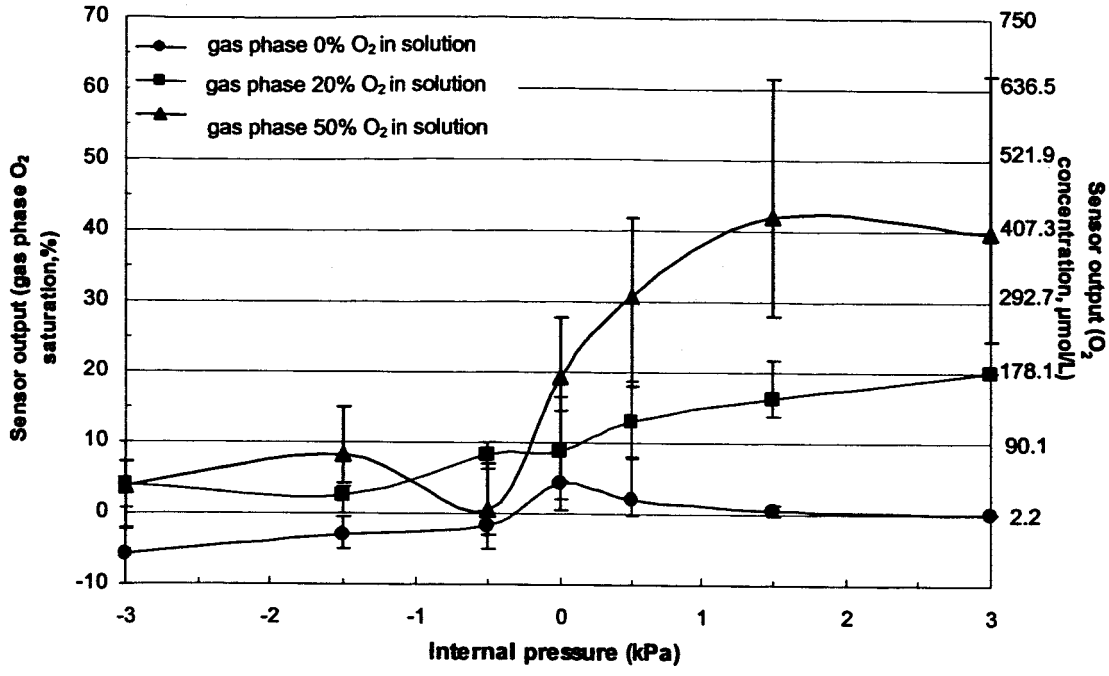

(a)

Figure 7 (a)

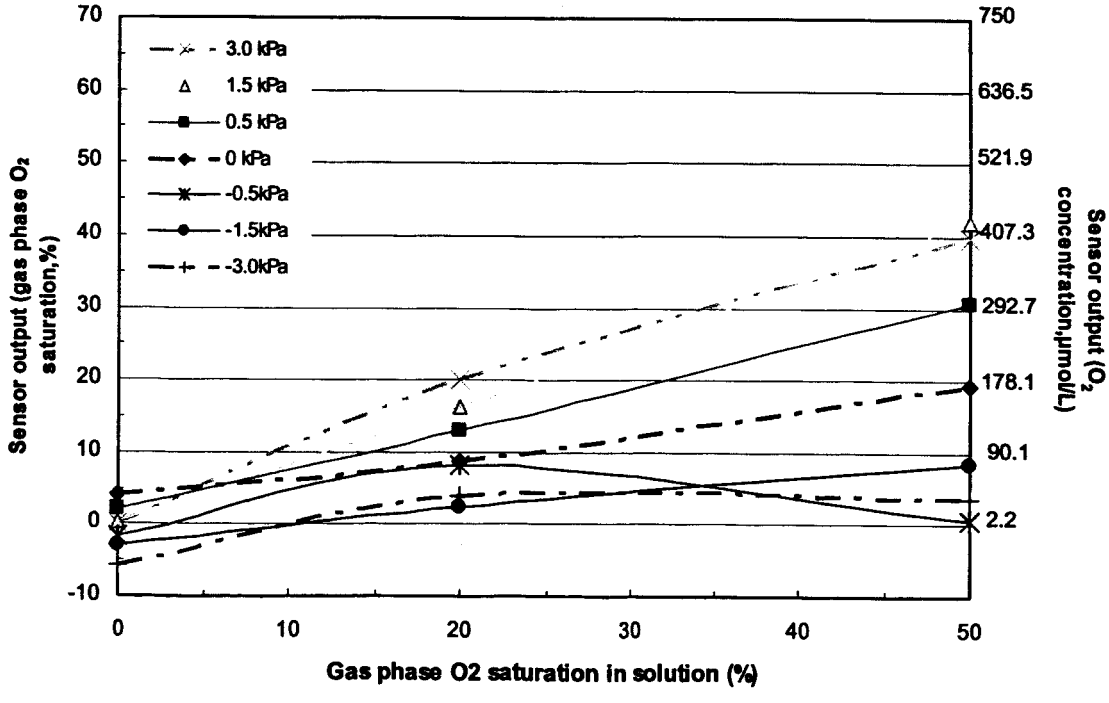

(b)

Figure 7 (b)

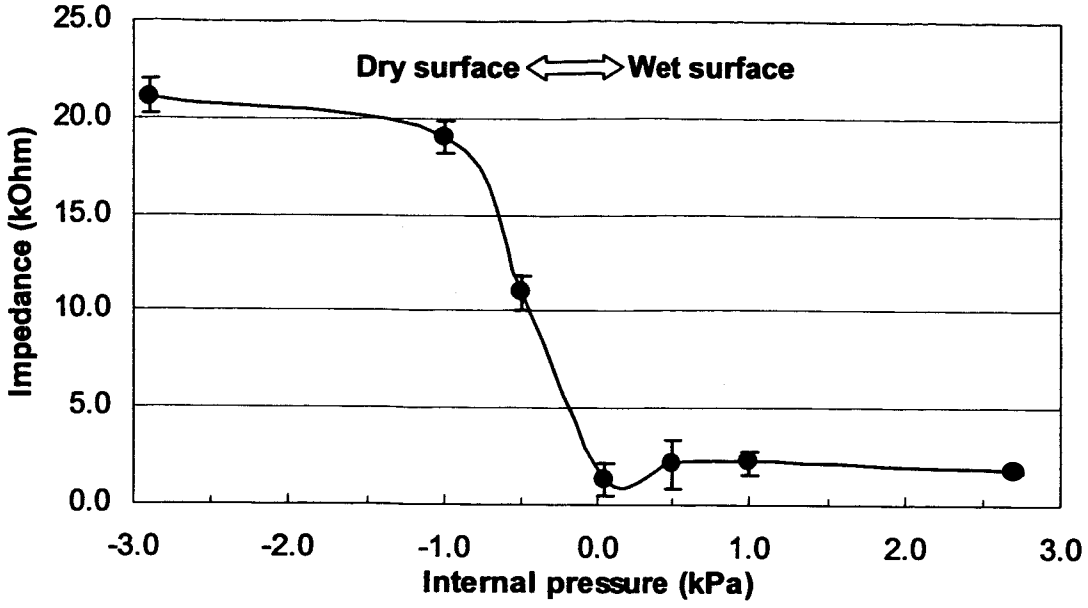
25.0
20.0
15.0
10.0
5.0
0.0
Impedance (kOhm)
Dry surface ⟺ Wet surface
-3.0
-2.0
-1.0
0.0
1.0
2.0
3.0
Internal pressure (kPa)

Figure 8